

A Simplified Model for Normal Mode Helical Antennas

Changyi Su, Haixin Ke, and Todd Hubing

Department of Electrical and Computer Engineering

Clemson University, SC 29634-3001, USA

csu@clemson.edu , hxkeucl@clemson.edu , hubing@clemson.edu

Abstract— Normal mode helical antennas are widely used for RFID and mobile communications applications due to their relatively small size and omni-directional radiation pattern. However, their highly curved geometry can make the design and analysis of helical antennas that are part of larger complex structures quite difficult. A simplified model is proposed that replaces the curved helix with straight wires and lumped elements. The simplified model can be used to reduce the complexity of full-wave models that include a helical antenna. It also can be used to estimate the performance of a helical antenna without full-wave modeling of the helical structure.

Index Terms— Helical Antennas, RFID.

I. INTRODUCTION

The helical antenna was introduced by John D. Kraus in 1946. Based on the far-field radiation pattern, a helical antenna operates in one of two principle modes: the normal mode with the maximum radiation perpendicular to the helix axis; or the axial mode with the maximum radiation in the direction of the axis [1]. The normal mode dominates when the diameter and axial length of the helix are much smaller than a wavelength. The radiation pattern of the normal mode helical antenna is omni-directional and generally similar to the pattern of a short dipole antenna. The self-resonant structure enables normal mode helical antennas to have radiation characteristics comparable to longer, straight-wire resonant dipole antennas [2]. Hence, normal mode helical antennas find many applications where the physical dimensions of the antennas are important, such as handsets [3], cellular phones [4]-[6] and RFID tags [7].

Unlike straight-wire dipole antennas, helical antennas are three-dimensional in structure and there is a lack of reliable formulas for their design

[8]. Most practical designs are the result of physical measurement trial-and-error, which is time-consuming and subject to errors introduced by the measurement facilities [4]. Therefore, numerical techniques are essential to helical antenna design and analysis [9], [10]. Helical antennas are mainly composed of curved surfaces and modeling these antennas using general purpose numerical tools requires mesh elements to be generated to fit the helical wire surfaces. This requires a large density of mesh elements and a great deal of computational resources. When modeling large systems that include a helical antenna, a significant portion of the computational effort may be devoted solely to the analysis of the helix, even when the helix is a small part of the total structure's volume.

In this paper, a simplified model is proposed to speed up the analysis of large structures containing helical antennas. In the simplified model, the helix is approximated by short straight wire segments connected by lumped elements representing the inductance of the helical turns. Theoretical calculations of the equivalent parameters are discussed. Nine different helix configurations are simulated using a general purpose full-wave modeling code to confirm the validity of the proposed model. The resonant frequency and input impedance of each configuration are examined. To further test the simplified model, two practical examples, an RFID antenna and a handset antenna, are also examined.

II. SIMPLIFIED MODEL

Fig. 1(a) shows the geometry of a helical dipole antenna. The helix is uniformly wound with a constant pitch, S . The radius of a helix can be uniform or tapered. In this paper, only uniform helices with constant radius, R , are considered. The helix's conductor is a wire of radius, a , with a

circular cross section. The antenna is fed at the midpoint of the coil winding. In this section, a simplified model of the helix is analyzed and analytical expressions for estimating the model parameters are established.

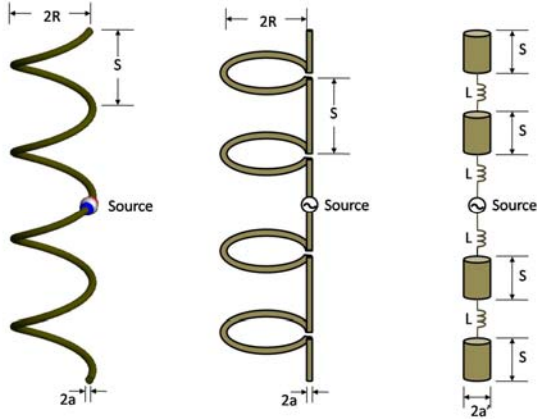


Fig. 1. (a) Helical antenna. (b) Wire-and-loop model. (c) Wire-and-inductor model.

It has been shown [1] that the helix can be approximated as a series of small loops and dipoles when the physical dimensions of the helix are much smaller than a wavelength. The equivalent wire-and-loop model for the helical antenna is shown in Fig. 1(b). The wire-and-loop model suggests that the axial ratio of the normal mode helical antenna can be expressed as

$$AR = \frac{E_\theta}{E_\phi} = \frac{2S\lambda}{(2\pi R)^2} = \frac{2S_\lambda}{C_\lambda^2} \quad (1)$$

where \$S_\lambda=S/\lambda\$ and \$C_\lambda=C/\lambda\$. \$C\$ is the circumference of the loop.

Most practical normal-mode helical antennas have an axial ratio greater than 1. In these antennas, the radiated field from the loops is smaller than the radiated field from the straight wire segments. We can generally neglect the radiation from the loops without incurring significant error. For example, if we require 2 dB of accuracy, we can still neglect the field radiated by the loops as long as,

$$\frac{E_\phi + E_\theta}{E_\theta} < 2 \text{ dB}. \quad (2)$$

Equations (1) and (2) imply that we can neglect the radiation from the loops as long as,

$$AR > 4. \quad (3)$$

From (1), it is clear that different axial ratios can be achieved by proper selection of the helix

dimensions. For example, with \$C_\lambda<0.1\$, \$AR>4\$ is satisfied when \$S_\lambda>0.02\$. The limits of the diameter and the pitch of the helix can be better expressed using the definition of pitch angle, e.g. in this case,

$$\tan(\alpha) = \frac{S}{C} > 0.2 \text{ or } \alpha > 11^\circ. \quad (4)$$

When the radiation from the loops can be neglected, they function like inductors. With this in mind, the wire-and-loop model can be further simplified by substituting inductors for the small loops as shown in Fig. 1(c). The proposed, simplified model consists of one straight wire segment per turn. Each segment is oriented vertically and has a length equal to the pitch of the helix. The segments are connected by lumped, inductive elements. The lumped elements do not increase the size of the mesh and do not significantly add to the computational complexity of the numerical analysis. Therefore, the simplified model requires considerably less computational resources to analyze than the original full-structure analysis.

In the original helix structure, the adjacent turns are coupled together via both mutual inductance and mutual capacitance. Since all the turns are coaxially oriented, some of the magnetic flux generated by one turn will pass through the neighboring turns. This part of flux induces a voltage that has the same polarity as the voltage drop caused by the self-inductance. In addition to the magnetic field coupling, electric field coupling also occurs between turns. The turn-to-turn capacitance provides an alternative current path that bypasses the loop and the straight wire. In the following sections, analytical expressions are derived that compensate for the mutual coupling that is missing in the simplified model.

A. Equivalent loop inductance

The parameters that need to be determined for the wire-and-inductor model in Fig. 1(c) include the equivalent inductance \$L\$ of a single turn, and the equivalent radius \$a'\$ of a short wire segment. The equivalent inductance includes the self-inductance \$L_{self}\$ of one turn and the mutual inductance \$M\$ coupled from its adjacent turns,

$$L = L_{self} + 2M. \quad (5)$$

The self inductance of a loop placed in free space is given by the double integral Neumann formula [13],

$$L_{self} = \frac{\mu_0}{4\pi} \oint \oint \frac{d\vec{l} \cdot d\vec{l}'}{r}. \quad (6)$$

Where μ_0 is the permeability of free space; and $d\vec{l}$ and $d\vec{l}'$ represent the differential elements separated by a distance, r . For a circular loop of wire, a closed form approximation for Eq. (6) is given by the following expression [13]:

$$L_{loop} = \mu_0 R \left[\ln\left(\frac{8R}{a}\right) - 2 \right] \quad (7)$$

where R is the loop radius and a is the wire radius.

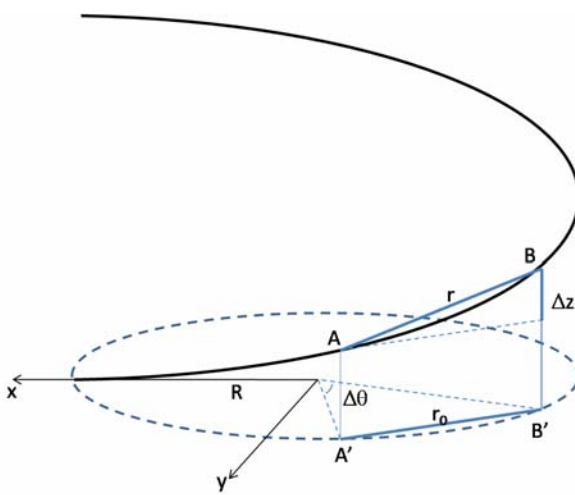


Fig. 2. Helical curve.

As shown in Fig. 2, the actual distance between any two points, A and B , on the helical curve is,

$$r = \sqrt{r_0^2 + \Delta z^2} \quad (8)$$

where r_0 is the distance between A' and B' obtained by projecting point A and B onto the x - y plane. Δz is the distance between points A and B in the z direction. When the pitch is small compared to the coil radius, the distance between A and B is approximately equal to that between A' and B' or $r \approx r_0$. Therefore, for a small pitch angle, Eq. (7) is a good approximation of the self inductance of a helix turn. However, as the pitch angle increases, Δz increases quickly. Consequently, the self inductance of a helix turn with a large pitch angle is much smaller than the inductance calculated by (7). Notice that for any point on the helix curve,

$$\frac{z}{R\theta} = \frac{S}{2\pi R}. \quad (9)$$

Therefore,

$$\Delta z = \frac{S}{2\pi R} R \Delta \theta. \quad (10)$$

Using the approximation,

$$r_0 \approx R \Delta \theta, \quad (11)$$

Eq. (8) becomes

$$r = r_0 \sqrt{\left(\frac{\Delta z}{r_0}\right)^2 + 1} \approx r_0 \sqrt{\left(\frac{S}{2\pi R}\right)^2 + 1}. \quad (12)$$

Substituting (12) into (6), the self inductance of a helix turn is given by,

$$\begin{aligned} L_{self} &= \frac{\mu_0}{4\pi} \oint \oint \frac{d\vec{l} \cdot d\vec{l}'}{r} \\ &\approx \frac{\mu_0}{4\pi} \oint \oint \frac{d\vec{l} \cdot d\vec{l}'}{r_0} \frac{1}{\sqrt{\left(\frac{S}{2\pi R}\right)^2 + 1}} \\ &= L_{loop} \frac{2\pi R}{\sqrt{(2\pi R)^2 + S^2}} \\ &= L_{loop} \cos(\alpha) \end{aligned} \quad (13)$$

The mutual inductance between two adjacent turns can be approximated by the mutual inductance between two coaxially oriented circular loops of radius R , separated by a distance S [13].

$$M = \frac{\pi \mu_0 R^4}{2(R^2 + S^2)^{\frac{3}{2}}}. \quad (14)$$

B. Equivalent wire radius

The capacitance of a wire with length l and radius a placed in free space is given by [14],

$$C_w = \frac{\pi \epsilon_0 l}{2 \ln\left(\frac{l}{a}\right)} \quad (15)$$

where ϵ_0 is the permittivity of free space. In Fig. 1(c), one helix turn is replaced by a short wire segment with a length equal to the helix pitch. The wire length is much shorter than the turn length; therefore, the total wire capacitance is reduced. To maintain the correct capacitance, the radius of the straight wire segments must be increased. The capacitance of the thicker wire should equal the capacitance of a helix turn. Therefore, the equivalent radius, a' , is obtained using the following expression:

$$\frac{S}{\ln\left(\frac{S}{a'}\right)} = \frac{l_{tot}}{\ln\left(\frac{l_{tot}}{a}\right)} \quad (16)$$

where $l_{tot} = \sqrt{(2\pi R)^2 + S^2}$.

The term on the left-hand side of (16) is the capacitance of a wire segment in the simplified model. The term on the right-hand side of (16) is the capacitance of a turn in the original helix. Eq. (16) is based on an assumption that the mutual capacitance between turns is negligible compared to the self capacitance of the wire. This is a reasonable assumption when the pitch angle satisfies the condition in Eq. (4).

III. VALIDATION OF THE SIMPLIFIED MODEL

In order to validate the simplified model described in the previous sections, the input impedances and the radiation patterns of helical antennas and the corresponding simplified models were calculated using a full-wave numerical modeling tool [17]. Since a normal mode helical antenna is generally designed to operate at its

resonant frequency, the performance of the simplified model near resonance is important. The evaluation was done by computing the relative differences in the calculated input resistance and resonant frequency. The error in the input resistance is defined as the ratio of the resistance difference over R_0 , the input resistance of the helical antenna at its resonant frequency f_0 . The error in the resonant frequency of the helical antenna is defined as the difference between the resonant frequency of the simplified antenna, f_1 , and the full helix, f_0 , divided by f_0 . Expressed as a percentage, the equations for these errors are indicated below:

$$Error(Re) = \frac{|R_0 - R|}{R_0} \times 100\% \quad (17)$$

$$Error(f) = \frac{|f_0 - f_1|}{f_0} \times 100\%. \quad (18)$$

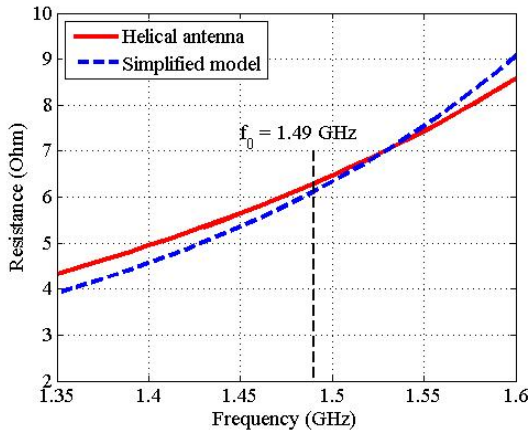
The geometrical parameters of the antennas evaluated are given in Table 1. The antennas are grouped in three sets. Within each set, one parameter was varied.

Table 1: Geometrical Parameters of Helical Antennas.

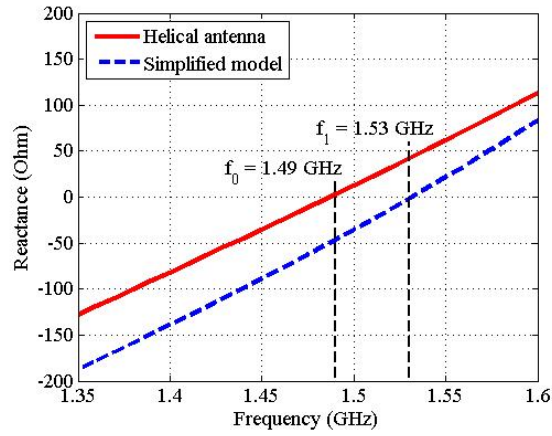
No	Geometry	Resonant frequency
Different wire radius		
1	$N = 10, R = 1 \text{ mm}, S = 1.68 \text{ mm}, \alpha = 15^\circ, a = 0.01 \text{ mm}$	2.89 GHz
2	$N = 10, R = 1 \text{ mm}, S = 1.68 \text{ mm}, \alpha = 15^\circ, a = 0.02 \text{ mm}$	2.97 GHz
3	$N = 10, R = 1 \text{ mm}, S = 1.68 \text{ mm}, \alpha = 15^\circ, a = 0.04 \text{ mm}$	3.08 GHz
Different pitch angle		
4	$N = 10, R = 2 \text{ mm}, S = 2.67 \text{ mm}, \alpha = 12^\circ, a = 0.02 \text{ mm}$	1.47 GHz
5	$N = 10, R = 2 \text{ mm}, S = 4.57 \text{ mm}, \alpha = 20^\circ, a = 0.02 \text{ mm}$	1.38 GHz
6	$N = 10, R = 2 \text{ mm}, S = 10.5 \text{ mm}, \alpha = 40^\circ, a = 0.02 \text{ mm}$	1.00 GHz
Different number of turns		
7	$N = 10, R = 2 \text{ mm}, S = 4.57 \text{ mm}, \alpha = 20^\circ, a = 0.02 \text{ mm}$	1.38 GHz
8	$N = 20, R = 2 \text{ mm}, S = 4.57 \text{ mm}, \alpha = 20^\circ, a = 0.02 \text{ mm}$	741 MHz
9	$N = 40, R = 2 \text{ mm}, S = 4.57 \text{ mm}, \alpha = 20^\circ, a = 0.02 \text{ mm}$	395 MHz

Table 2: Equivalent Parameters of Simplified Models.

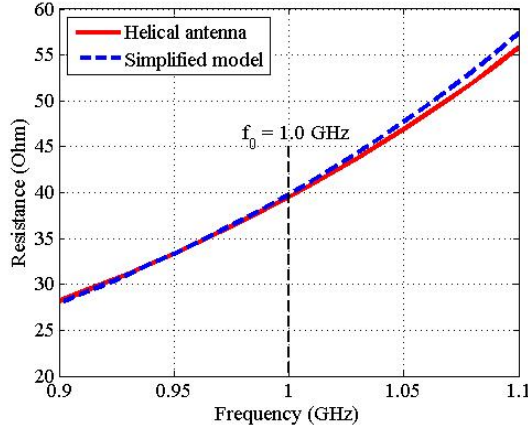
No	Equivalent parameters	Error (Re) (%)	Error (<i>f</i>) (%)
1	$a' = 31.5a, L = 6.21\text{nH}$	2.2	1.3
2	$a' = 18.9a, L = 5.35\text{nH}$	1.5	1.3
3	$a' = 11.3a, L = 4.51\text{nH}$	0.7	1.6
4	$a' = 34.8a, L = 13.2\text{nH}$	3.2	2.7
5	$a' = 24.7a, L = 11.5\text{nH}$	4.0	0.1
6	$a' = 7.11a, L = 9.07\text{nH}$	0.6	1.0
7	$a' = 24.7a, L = 11.5\text{nH}$	4.0	0.1
8	$a' = 24.7a, L = 11.5\text{nH}$	1.4	1.7
9	$a' = 24.7a, L = 11.5\text{nH}$	3.2	2.2



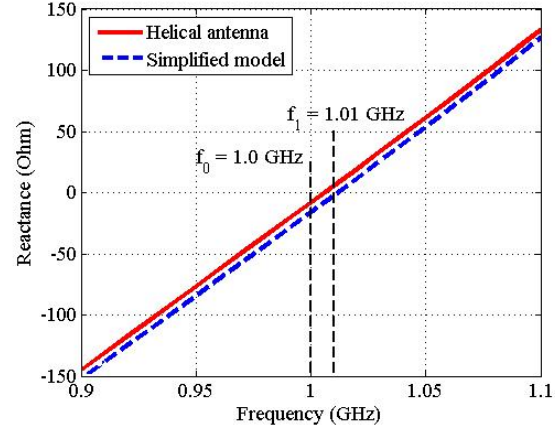
(a) Case 4: Input resistance.



(b) Case 4: Input reactance.



(c) Case 6: Input reactance.



(d) Case 6: Input reactance.

Fig. 3. Input impedance for Cases 4 and 6.

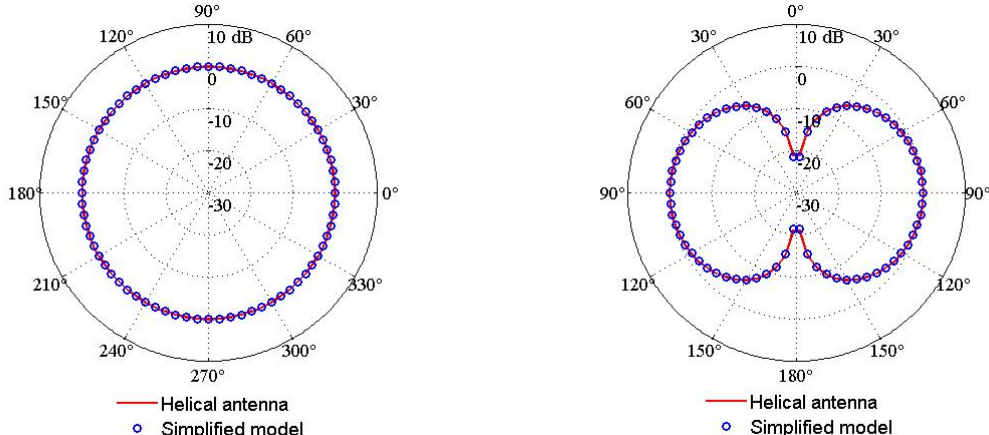


Fig. 4. Radiation patterns for Case 4: (a) Azimuth plane field pattern (b) Elevation plane field pattern.

Table 3: CPU-time and memory usage.

No	CPU-time (Second)		Memory-usage (MBtye)	
	Original model	Simplified model	Original model	Simplified model
1	4.28	0.4	14.8	0.54
2	4.23	0.65	14.8	0.75
3	4.95	0.64	16.9	0.96
4	20.8	0.46	65.6	0.72
5	24.9	0.46	74.4	0.82
6	44.3	2.37	115.5	2.8
7	24.9	0.43	74.4	0.82
8	146.4	1.51	311.3	2.67
9	506	5.42	890	9.54

The relative errors in the input resistance and resonant frequency for each case are listed in Table 2. The input resistances at the resonant frequency of the simplified model are in reasonable agreement (within 5%) with values calculated for the full helix in all cases. The good agreement suggests that the analytical formulas (13) - (16) are sufficiently accurate near resonance for the helical antenna geometries evaluated. Table 3 shows the computation time and the amount of memory per frequency required to analyze each original helical antenna and its simplified model. The simplified model significantly reduces both the CPU-time and the memory usage.

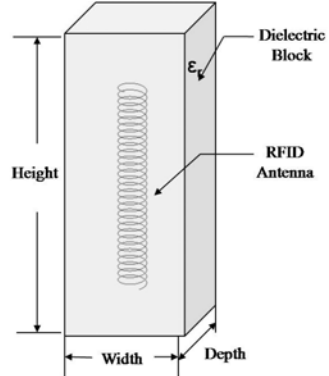


Fig. 5. An RFID antenna embedded in a dielectric block.

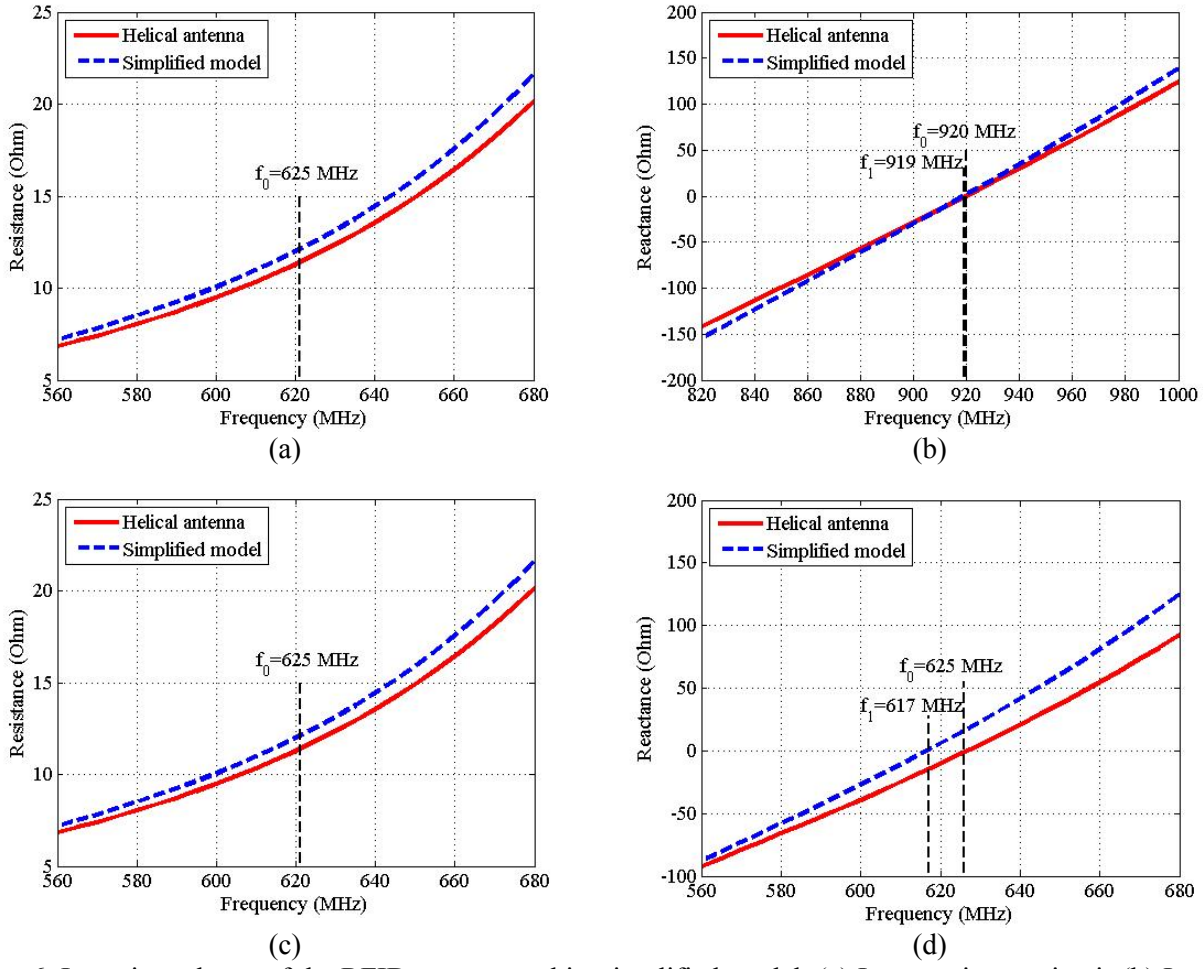


Fig. 6. Input impedance of the RFID antenna and its simplified model: (a) Input resistance in air (b) Input reactance in air (c) Input resistance in dielectric (d) Input reactance in dielectric.

One application of the simplified model is RFID antennas, which are widely used for identification and tracking of objects using radio waves. Recently, tire makers have begun embedding RFID tags in some of their tires to enable them to be tracked electronically. These tags often employ helical antennas embedded in a dielectric material as illustrated in Fig. 5. In this example, the antenna is designed to resonate at around 920 MHz. The parameters of the helix are: $N = 106$ turns, $R = 0.5$ mm, $S = 0.833$ mm, $a = 0.09$ mm. The dimensions of the dielectric block are $97 \times 11 \times 11$ mm. The relative permittivity of the dielectric is 4.0.

The input impedance of both the RFID antenna and the simplified model are calculated for the antenna in air and the antenna in the dielectric block (Fig. 6). The difference between the helix and simplified model calculations of the

input impedance is less than 5% for both the RFID antenna in air and in the dielectric block.

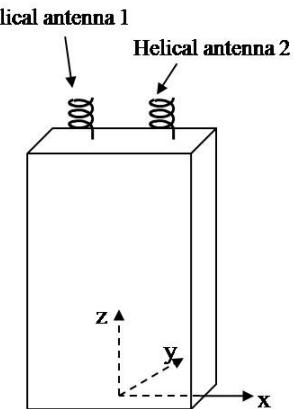
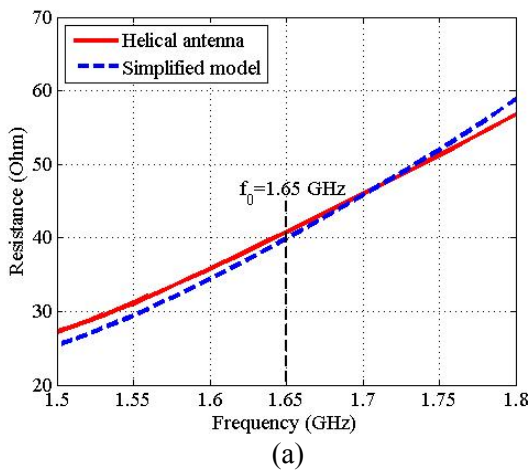


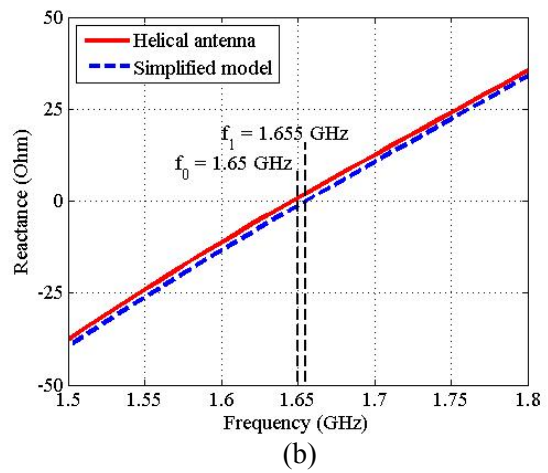
Fig. 7. Mobile handset and coordinate system.

In order to further test the proposed model, a practical helical antenna design [3] for mobile handsets was also simulated. In this design, two helical antennas are mounted on top of a metal box ($10 \times 4.8 \times 1.67$ mm) and separated by 3.125 cm (Fig. 7). Antenna 1 is excited and Antenna 2 is connected to a $50\text{-}\Omega$ load. The helical antenna array is tuned to resonate at about 1.65 GHz. The antenna parameters are: $N = 2.6$ turns, $S = 9.94$ mm, $R = 2.1$ mm, $a = 0.28$ mm. The simplified model requires an integer number of turns. Therefore, the number of turns was set to 3 in this simulation. The simulation results are shown in

Figs. 8 and 9. The input resistance of the simplified model is close to that of the helical antenna near the resonant frequency. The error in the resonant frequency is only 1%. The radiation pattern predicted by the simplified model is identical to that of the helical antenna in both azimuth and elevation planes. The good agreement demonstrates that the proposed model is not only suitable for dipole-helical antennas, but it can be also applied to monopole-helical antennas.

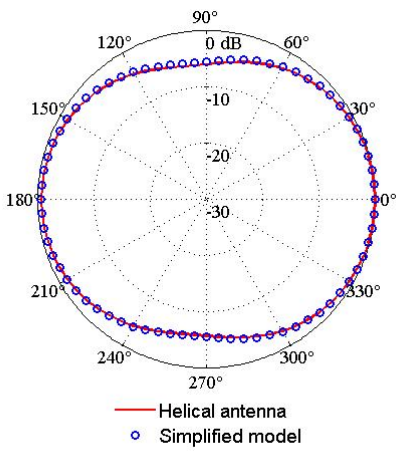


(a)

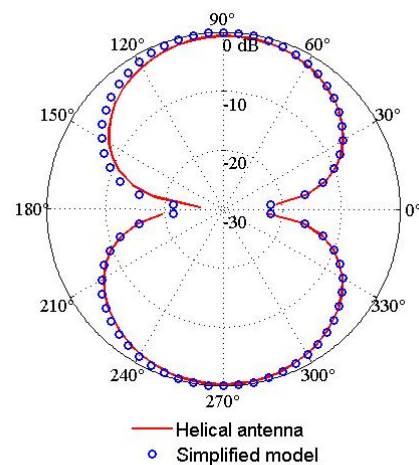


(b)

Fig. 8. Input impedance of the helical antenna of the handset: (a) Input resistance (b) Input reactance.



(a)



(b)

Fig. 9. Radiation patterns for the handset helical antenna in the Azimuth plane: (a) E_θ (b) E_ϕ .

IV. CONCLUSION

A simplified model for helical antennas has been proposed. In the model, the highly curved structure of the helix is replaced with a straight-wire and inductor structure. The number of elements required to model the helix is significantly reduced; and therefore, analysis of the simplified model uses much less computational resources than analysis of the full helix.

REFERENCES

- [1] J. D. Kraus, *Antennas*, 2nd ed., McGraw-Hill, 1988.
- [2] Y. Hiroi, K. Fujimoto, "Practical usefulness of normal mode helical antenna," *IEEE AP-S Int. Symp.*, pp. 238-241, 1976.
- [3] H. T. Hui, "Practical dual-helical antenna array for diversity/MIMO receiving antennas on mobile handsets," *IEE Proceeding, Microwaves, Antennas and Propagation*, vol. 152, no. 5, pp. 367-372 2005.
- [4] M. M. Faiz and P. F. Wahid, "Microstrip line matched normal mode helical antenna for cellular communication," *Southeastcon'98, Proceedings, IEEE*, pp. 182-185.
- [5] H. Morishita, Y. Kim, H. Furuuchi, K. Sugita, Z. Tanaka and K. Fujimoto, "Small balance-fed helical dipole antenna system for handset," *51st Vehicular Technology Conference (VTC) Proceedings*, Tokyo, vol. 2, pp.1377 – 1380, May 15-18, 2000.
- [6] K. Noguchi, S. Betsudan, T. Katagi, and M. Mizusawa, "A compact broad-band helical antenna with two-wire helix," *IEEE Trans. Antennas Propagat.*, vol. 51, no. 9, pp. 2176-2181, 2003.
- [7] Y. Yamada, W. G. Hong, W. H. Jung and N. Michishita, "High gain design of a very small normal mode helical antenna for RFID tags," *IEEE Region 10 Conference*, pp. 1-4, 2007.
- [8] A.R. Djordjevic, A.G. Zajic, M.M. Ilic, and G.L. Stuber, "Optimization of helical antennas," *IEEE Trans. Antennas Propagat.*, vol. 48, pp. 107-105, 2007.
- [9] G. Lazzi, and O. P. Gandhi, "On modeling and personal dosimetry of cellular telephone helical antennas with the FDTD codes," *IEEE Trans. Antennas Propagat.*, vol. 46, pp. 525-530, 1998.
- [10] E. D. Caswell, "Analysis of a helical antenna using a moment method approach with curved basis and testing functions," M. Sc. Thesis, Virginia Polytechnic Institute, 1998.
- [11] C. A. Balanis, *Antenna Theory – Analysis and Design*, 3rd ed., John Wiley & Sons Inc., 2005.
- [12] S. Ramo, J. R. Whinnery and T. V. Duzer, *Fields and Waves in Communication Electronics*, New York, J. Wiley, 1965.
- [13] S. A. Schelkunoff and H. T. Friis, *Antennas: Theory and Practice*, John Wiley & Sons Inc., 1952.
- [14] F. M. Tesche, et al., *EMC Analysis Methods and Computational Models*, Wiley-IEEE, 1997.
- [15] A. J. Palermo, "Distributed capacity of single layer coils", *Proc. IRE*, vol. 22, pp.897-903, 1934.
- [16] G. H. Brown and O. M. Woodward, Jr., "Experimentally determined impedance characteristics of cylindrical antennas," *Proc. IRE*, vol. 33, pp. 257-262, 1945.
- [17] FEKO, <http://www.feko.info>.



Changyi Su received her B.Eng. degree from Xian University of Technology, Xian, China and her M. Eng. degree from Nanyang Technological University, Singapore in 1993 and 2001, respectively. She is working toward the Ph.D. degree at Clemson University, Clemson, SC. Her research interests include electromagnetic modeling, and computational electromagnetics.



Haixin Ke received the B.S. and M.S. degrees from Tsinghua University, Beijing, China, in 1998 and 2001, respectively, and the Ph.D. degree from the University of Missouri, Rolla, in 2006, all in electrical engineering. From 2006 to 2009, he worked as a Postdoctoral Researcher at Clemson University, Clemson, SC. He is currently a Postdoctoral Research Associate at Washington University in St. Louis, MO. His research interests include computational electromagnetics, electromagnetic compatibility, and microwave/optical imaging.



Todd H. Hubing received a B.S. degree from MIT in 1980, an M.S. degree from Purdue in 1982, and a Ph.D. degree from North Carolina State in 1988, all in electrical engineering. From 1982 to 1989, he worked for IBM in Research Triangle Park, NC. In 1989, he joined the faculty at the University of Missouri-Rolla; and in 2006, he moved to Clemson University, where he is currently the Michelin Professor of Vehicle Electronics.

Prof. Hubing is a member of the Board of Directors of the IEEE EMC Society and a past-president of that society. He is a Fellow of the IEEE and a Fellow of the Applied Computational Electromagnetics Society.